Radiation Tolerance of High-Resistivity LBNL CCDs

Kyle Dawson, Chris Bebek, John Emes, Steve Holland, Sharon Jelinsky, Armin Karcher, William Kolbe, Nick Palaio, Natalie Roe, Koki Takasaki and Guobin Wang
Lawrence Berkeley National Laboratory
One Cyclotron Rd
Berkeley, CA 94720

Abstract— **Thick, fully-depleted p-channel charge-coupled devices (CCDs) have been developed at the Lawrence Berkeley National Laboratory (LBNL). These CCDs have several advantages over conventional n-channel CCDs, including enhanced quantum efficiency and reduced fringing at near-infrared wavelengths, a small point spread function, and improved radiation tolerance. Here we report results from the irradiation of CCDs with 12.5 and 55 MeV protons at the LBNL 88-Inch Cyclotron. These studies indicate that the CCDs still perform well after irradiation, even in the parameters in which significant degradation is expected: charge transfer efficiency, dark current, and isolated hot pixels. As expected, the radiation tolerance of the LBNL CCDs is significantly improved over conventional n-channel CCDs currently employed in space-based telescopes such as the Hubble Space Telescope (HST).**

Index Terms— **Astrophysics and Space Instrumentation, Radiation Damage Effects**

I. Introduction

The SuperNova/Acceleration Probe (SNAP) is a proposed space-based telescope dedicated to the study of dark energy through observations of type Ia supernovae (SNe) and a deep, wide area weak lensing survey [1]. SNAP observations will begin with a deep survey covering two 7.5 square degree fields over a period of 22 months. The goal of this deep survey is to discover and obtain light curves and spectroscopic confirmation of 2000 SNe in the redshift range $0.3 < z < 1.7$, with exquisite control of systematic errors. Following the SN survey, SNAP will expand the sky coverage to generate a high fidelity weak lensing map to study the growth of large scale structure. In order to meet weak lensing science requirements, 12 months of observations are planned to provide a galaxy density of at least 100/arcminute^2 over 1000 square degrees, with an option to extend the weak lensing survey to 4000 square degrees over an additional three years.

The telescope is designed with a 0.7 square degree instrumented field of view divided evenly between 36 CCDs and 36 HgCdTe detectors. The focal plane will be passively cooled to 140 K with nine fixed filters covering the wavelength range 400 nm to 1700 nm. With a diffraction limited point spread function (PSF) of 0.1 arcseconds at 800 nm and zodiacal-dominated background, SNAP will have significantly improved resolution and decreased contamination from sky background compared to ground based telescopes.

Further author information: E-mail kdawson@lbl.gov

The SNAP focal plane design uses thick, fully depleted CCDs designed at LBNL [2] for visible to near IR observations covering six bandpass filters. As a space-based telescope, these detectors will be exposed to significant radiation, primarily from solar protons. In this paper we investigate the effects of radiation on SNAP CCDs in order to qualify them for use in a space mission. In §II we describe the SNAP CCDs and the specifications for performance. The space environment and expected radiation exposure are discussed in §III. Irradiation at the 88-inch Cyclotron at LBNL is described in §IV and CCD performance after irradiation is reported in §V. Finally, we present an interpretation of the results in the context of the SNAP mission in §VI and the conclusion in §VII.

II. CCD Requirements

SNAP CCDs have been designed for back-illumination on 200 μm thick, fully-depleted, high-resistivity silicon. A factor of ten increase in thickness over conventional CCDs provides vastly improved sensitivity toward wavelengths of 1μm and negligible fringing effects caused by multiply reflected photons inside the silicon [3], [4]. The CCDs are depleted through application of a substrate bias voltage across the full thickness. The spatial resolution is improved by increasing the bias voltage up to 200 V [2]. The SNAP focal plane will be populated with 36 LBNL CCDs, each consisting of 3512×3512 10.5 μm pixels.

The objectives of the SNAP experiment will be to extract point-source SNe from diffuse host galaxies and to resolve distant galaxies for weak lensing studies. The specifications for CCD performance are therefore governed by requirements for preservation of the point spread function (PSF), charge transfer efficiency (CTE) and signal-to-nose ratio. In Table I we list the specifications for the SNAP CCDs. As can been seen in the table, each of these requirements has been met in the current design of SNAP style devices before radiation exposure.

CCD performance is expected to degrade in a radiation environment due to bulk damage through non-ionizing energy loss (NIEL) of high-energy incident particles. The major bulk damage in n-channel CCDs is caused by traps generated in the formation of phosphorus-vacancy centers. This bulk damage manifests itself through increased dark current, isolated hot pixels, and decreased charge transfer efficiency. The LBNL p-channel CCDs are fabricated on high-resistivity n-type silicon.

1-4244-0561-0/06/$20.00 ©2006 IEEE.

TABLE I

SPECIFICATIONS FOR SNAP CCDS

Quantity	Requirement	Achieved (pre-irradiation)
Wavelength Coverage	$400 - 1000$ nm	$400 - 1000$ nm
Quantum	$> 80\%$ at $600 - 950$ nm	$> 80\%$ at $600 - 950$ nm
Efficiency	$> 50\%$ at 1000 nm	$> 50\%$ at 1000 nm
Readout Time	30 seconds	30 seconds
Read Noise	6 e^-	4 e^-
Diffusion (RMS)	6μm	4μm
Defect Pixels[a]	TBD	$< 0.1\%$
Dark Current[a]	100 e^-/hr	$3 - 4$ e^-/hr
Serial CTE[a]	TBD	0.999 999
Parallel CTE[a]	TBD	0.999 999

[a]expected to deteriorate with irradiation

The channel is boron implanted, leaving an extremely small concentration of phosphorus compared to n-channel CCDs. It is therefore not expected that the phosphorus-vacancy centers will affect the radiation tolerance of the LBNL CCDs, rather divacancy states will dominate [5].

III. SPACE ENVIRONMENT AND EXPECTED DOSE

The SNAP satellite will be placed in orbit at the L2 Lagrange point, approximately 1.5×10^6 km from the earth. At this distance, solar protons dominate the total radiation dose. To estimate the total exposure at L2, we use the model for emission of solar protons [6] and the Space Environment Information System (SPENVIS) [7] as a first order approximation. In SPENVIS, the solar model is simplified as a cycle with seven years at maximum with constant exposure and four years at minimum with no exposure. The model provides a statistical estimate of the fluence as a function of confidence interval based on data from the past three solar cycles. A simple shielding model is used in which a spherical Al shell surrounds the detectors.

Assuming a five year extended mission with a January 1, 2014 launch date, we use a 95% confidence limit for our calculations. Figure 1 shows the spectrum of protons incident on the detector at L2 for various shield thicknesses. Similarly, Figure 2 reports the integrated NIEL as a function of shield thickness.

Because of structure within the satellite, the shielding thickness depends on the path to the detector, varying by almost a full order of magnitude over the full range of angles of incidence. The current SNAP satellite design has an average shielding equivalent to about 40 mm of Al shielding around the focal plane, taken over the 4π solid angle of the instrument. The minimum shielding is equivalent to 9 mm of Al. For this worst case, we would expect a displacement damage dose of 3×10^7 MeV/g(Si). Using the average Al thickness in a more realistic interpretation of the effects of shielding, the dose is significantly smaller, only 5×10^6 MeV/g(Si). Assuming a NIEL factor of 8.9×10^{-3} Mev/g/cm^2 for 12.5 MeV protons [8], the equivalent dose for 9 mm of Al shielding is 3.4×10^9 protons/cm^2 and for 40 mm of Al shielding is 5.6×10^8 protons/cm^2. We report results of the radiation tolerance of the SNAP CCDs treating 9 mm shielding as an overly pessimistic worst case scenario and 40 mm Al shielding as a "nominal" value.

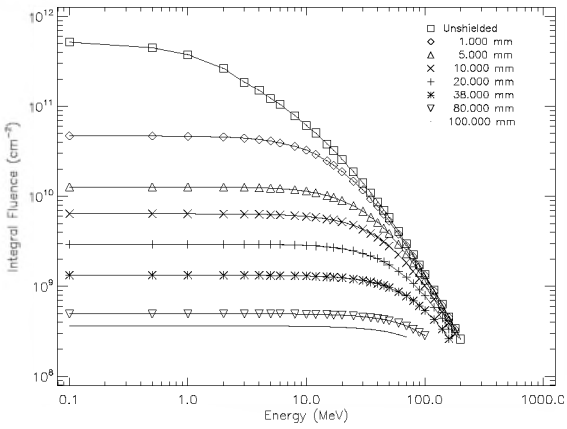

Fig. 1. Spectrum of incident particles for various shielding thicknesses. Results indicate 95% upper limits assuming a five year mission with launch date January 1, 2014. A shielding thickness of 9 mm is considered as a worst case scenario while a shielding thickness of ~ 40 mm is the average amount of shielding of the SNAP focal plane.

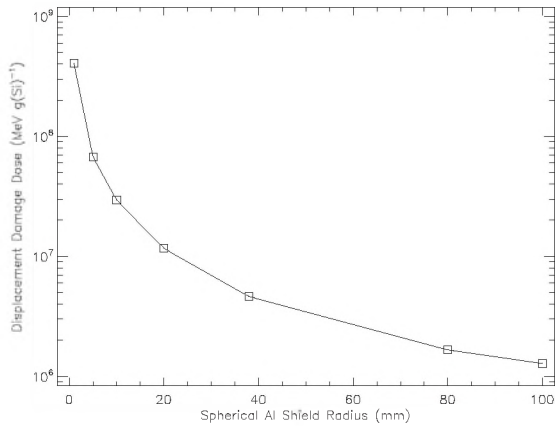

Fig. 2. NIEL damage as a function of shielding thickness. Results indicate 95% upper limits assuming a five year mission with launch date January 1, 2014. A shielding thickness of 9 mm is considered as a worst case scenario while a shielding thickness of ~ 40 mm is the average amount of shielding of the SNAP focal plane.

IV. Irradiation at 88-inch Cyclotron

Each CCD was characterized before irradiation, with performance very similar to that described in Table I. Charge transfer efficiency (CTE) was measured using ^{55}Fe stacking plots for both parallel and serial transfers. Gain conversion from ADU to e^- was also determined using ^{55}Fe images. Dark current was measured in 10 minute exposures, using a simple iterative clipping algorithm to remove cosmic ray contamination. Ten dark images were taken successively and median combined to generate a high signal-to-noise dark image, free of cosmic rays. A simple object-finding algorithm was used to detect residual hot pixels caused by a clustering of mid-level traps in this median combined image. Very rarely was even a single individual hot pixel identified in a dark image; more common was the occasional hot column caused by a minor clock short or back side defect. For a more detailed account of clock shorts and back side defects, see Holland et al (2005) [2].

To simulate radiation exposure in the space environment, several CCDs were taken to the LBNL 88-inch Cyclotron for proton irradiation on January 30, 2006. A second round of CCDs were irradiated on July 14, 2006. Full 3512x3512 pixel SNAP CCDs were used in the irradiation as well as smaller format CCDs with design otherwise identical to the SNAP CCDs.

Devices were irradiated unbiased with all signals shorted together at room temperature using 55 MeV and 12.5 MeV protons. With the use of brass shielding, the four quadrants of a SNAP CCD were individually exposed to doses of 5×10^9, 1×10^{10}, 5×10^{10} and 1×10^{11} protons/cm^2 at 55 MeV. Four small format SNAP CCDs were left unshielded during irradiation, receiving exposures of 5×10^9, 1×10^{10}, 5×10^{10} and 1×10^{11} protons/cm^2 at 12 MeV, respectively. In addition to those CCDs irradiated at room temperature, a SNAP style CCD was irradiated inside the dewar at 133 K during normal operating conditions. Nominal bias and clocking voltages produced a continual readout at 70 kHz during the exposure. A brass shield was placed in front of the CCD inside the dewar using an adapted ^{55}Fe plunger. From outside the dewar, the shield could be moved into three different positions, resulting in exposures to three different regions of the CCD. Three regions of this CCD respectively received doses of 5×10^9, 1×10^{10} and 2×10^{10} protons/cm^2 at 12 MeV.

V. Results

Dark current can fill traps, resulting in better CTE measurements than would be obtained at lower dark current levels, so we allowed 4 weeks for the dark current to fall to a low level following the irradiation The warm-irradiated CCDs were again characterized as described above with the primary objective of determining the degradation of CTE as a function of dose and energy. The cold-irradiated CCD was maintained at 133 K for seven weeks following irradiation. Dark and ^{55}Fe images were collected on a regular basis, beginning only 3 days after the irradiation. The primary purpose of the cold-irradiation and analysis was to determine the evolution of CTE, dark current, and isolated hot pixels at normal operating conditions over an extended period, as well as to examine the effects of an anneal to room temperature, an analysis not possible with the warm irradiated CCDs. All CTE measurements were carried out at a readout frequency of 70 kHz at a temperature of -140 C with an ^{55}Fe density of approximately one X-ray per 80 pixels for the warm-irradiated CDDs and one X-ray per 270 pixels for the cold-irradiated CDDs.

A. Energy Dependence of CTE Degradation

As a simple test of the validity of the NIEL approximation of CTE degradation, CCDs irradiated at 55 MeV were compared to CCDs irradiated at 12.5 MeV. As can be seen in Table II, the damage factor describing serial CTE degradation is nearly identical for both energies. The damage factor was observed to be 15% larger in parallel CTE in the case of the 55 MeV irradiation, a relatively minor difference.

B. Scaling of CTE with Dose

The CTE of the warm-irradiated SNAP CCDs was analyzed and compared over the full range of exposure levels. Results of the degradation of parallel CTE are shown in Figure 3(a). As a standard of comparison, we also include the results of CTE testing on conventional n-channel CCDs from e2v, Inc. [9]. The n-channel CCDs are intended to be used in the Wide Field Camera 3 (WFC3) on HST and were irradiated using 63 MeV protons with a fluence of 2.5×10^9 protons/cm^2 and 5×10^9 protons/cm^2, equivalent to 2.5 and 5.0 years in the HST orbit. Assuming a NIEL of 3.7×10^{-3} MeV/g(Si) for 63 MeV protons [8], the equivalent dose at 12.5 MeV is 1.04×10^9 protons/cm^2 and 2.08×10^9 protons/cm^2.

Serial CTE vs dose is shown in Figure 3(b). As can be seen in the figure, the warm-up to room temperature seems to have caused a reverse anneal, resulting in approximately a factor of two increase in the charge transfer inefficiency. The cause of the reverse anneal is still under investigation, but similar behavior has been observed in CCDs used in the Chandra telescope [10]. It has been demonstrated that irradiation produces only negligible degradation of serial CTE in the n-channel e2v devices and results are not included here.

TABLE II
CTE degradation at 12.5 MeV and 55 MeV

Energy	Transfer Direction	Dose protons/cm^2	CTI	NIEL MeV/g(Si)	Damage Factor CTI/Dose/NIEL
12.5 MeV	parallel	1×10^{11}	3.8×10^{-4}	8.9×10^{-3}	4.3×10^{-13}
55 MeV	parallel	1×10^{11}	2.0×10^{-4}	4.1×10^{-3}	4.9×10^{-13}
12.5 MeV	serial	1×10^{11}	2.8×10^{-4}	8.9×10^{-3}	3.1×10^{-13}
55 MeV	serial	1×10^{11}	1.3×10^{-4}	4.1×10^{-3}	3.2×10^{-13}

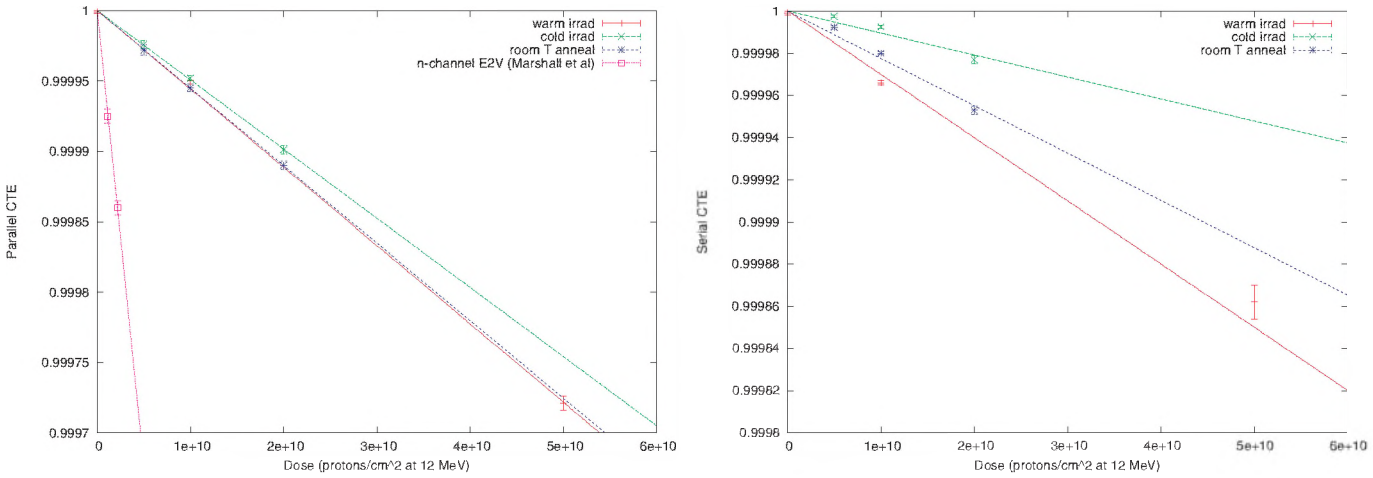

(a) Parallel CTE

(b) Serial CTE

Fig. 3. a) Parallel CTE as a function of dose for SNAP CCDs and n-channel e2v CCD similar to that used in ACS on HST with best fit linear approximation for each case. b) Serial CTE as a function of dose for SNAP CCDs with best fit linear approximation.

C. Generation of Hot Pixels

Median-stacked, cosmic ray-cleaned dark images from before irradiation were compared to similar darks taken following irradiation in the cold-irradiated SNAP CCD. Using a simple scheme to subtract the pre-irradiation image from the post-irradiation image, a map was generated to identify residuals produced as a result of the irradiation. Hot isolated pixels in this residual map represent spikes in dark current, created from clustering of bulk defects and will be flagged in science images. Hot pixels are located and counted by identifying pixels that lie a certain threshold above the mean background level. The number density of these hot pixels as a function of threshold is shown in Figure 4.

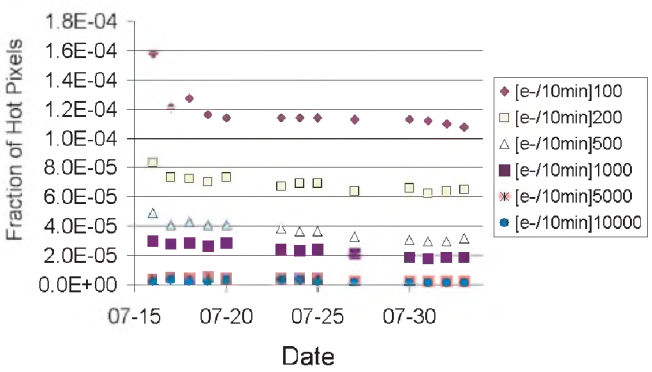

Fig. 4. Isolated hot pixels after irradiation with 2×10^{10} protons/cm^2.

With a threshold of 100 e$^-$ in a ten minute exposure, the density of hot pixels is 1.13×10^{-4} for a dose of 2×10^{10} protons/cm^2. The density of hot pixels is 3.1×10^{-5} with a threshold of 500 e$^-$ in a ten minute exposure.

A similar experiment was conducted using n-channel e2v CCDs designed for WFC3. These CCDs were exposed to 63 MeV protons at a total fluence of 2.5×10^9 protons/cm^2, equivalent to an exposure at 12.5 MeV of 1.04×10^9 protons/cm^2. After the anneal, a fraction of 2.5×10^{-3} hot pixels were detected at a threshold of 26 e$^-$/10 min [11]. Applying this threshold to the LBNL data, and scaling the result to the same dose, we find a fraction of 2.0×10^{-5} hot pixels before the anneal and 1.3×10^{-6} hot pixels after the anneal.

The improvement by over three orders of magnitude in the rate of hot pixels for the LBNL CCDs relative to the e2V CCDs is at least in part due to the different operating temperatures for the SNAP (-133C) and WFC3 (-83C) focal planes. The rate of hot pixels in the e2v CCDs was observed to decline by two orders of magnitude as operating temperature was reduced from -65 C to -90 C. The hot pixel rate in LBNL CCDs has not been studied at the higher temperature of the WFC3 instrument.

D. Evolution of Dark Current

The level of dark current (DC) as a function of time can be found in Figure 5.

The evolution of dark current is well described by a two term exponential decay.

$$DC = A_0\, e^{-t/t_0} + A_1\, e^{-t/t_1} + C \qquad (1)$$

The model is fit to the data, and best-fit parameters can be found in Table III. The curve described by the best-fit model for each dose is found in Figure 5. Examination of the best fit parameters indicate that the dark current scales roughly with dose before the anneal and that the time constants are not dose dependent. It is also evident from Table III that the decay time constants are short compared to the mission lifetime. A room temperature anneal appears to initiate a second decay in the dark current with time constants similar to those observed immediately following the exposure.

TABLE III

PARAMETERS DESCRIBING EVOLUTION OF DARK CURRENT

Dose	A_0 (e^-/px/hr)	t_0 (hr)	A_1 (e^-/px/hr)	t_1 (hr)	C (e^-/px/hr)
Before Room Temperature Anneal					
5×10^9	6500 $\pm$40.7	61.9 $\pm$0.7	1050 $\pm$27.8	331 $\pm$9.5	113 $\pm$4.1
1×10^{10}	12900 $\pm$136	63.4 $\pm$1.2	2100 $\pm$108	328 $\pm$19.5	228 $\pm$20.0
2×10^{10}	24300 $\pm$470	61.5 $\pm$1.3	4200 $\pm$156	311 $\pm$12.1	466 $\pm$20.5
Following Room Temperature Anneal					
1×10^{10}	398 $\pm$90	52.8 $\pm$15	142 $\pm$47	194 $\pm$37	58 $\pm$3
2×10^{10}	730 $\pm$44	59.6 $\pm$4.9	178 $\pm$21	288 $\pm$32	94 $\pm$2.5

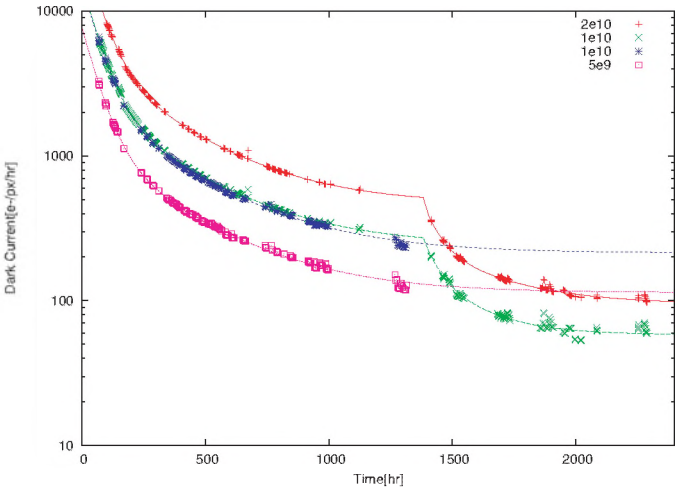

Fig. 5. Evolution of Dark Current in cold-irradiated device.

VI. DISCUSSION

Both the parallel and serial CTE scale roughly as expected as a function of proton energy, providing evidence that the NIEL approximation of CTE degradation is fairly robust. Assuming the NIEL approximation is valid, we extrapolate the results of the 12.5 MeV irradiation to model the effects of exposure at the L2 Lagrange point.

An analysis of the CTE shows a significantly improved radiation tolerance of the LBNL CCDs over the n-channel e2v CCD intended for WFC3. Given the model for radiation exposure of HST, the WFC3 CCDs are expected to degrade to a parallel CTE of 0.999 925 after 2.5 years in orbit when measured using the ^{55}Fe method. On the other hand, when extrapolated to the dose expected in the worst case scenario, the SNAP CCDs are still expected to perform with a parallel CTE of 0.999 978 after five years in orbit. With a mission twice as long and an overly pessimistic estimate of shielding, the SNAP CCDs are expected to have a lower loss of parallel CTE by a factor of three. The serial CTE is somewhat better, with a predicted value of 0.999 991 after 5 years, improving by a factor of two if the device is never annealed. If the more realistic nominal dose is assumed, the performance is significantly better, with a parallel CTE of 0.999 996 and a serial CTE of 0.999 998 after five years.

As argued in §V-C, the SNAP CCDs are quite resilient to hot pixels after irradiation. Hot pixels effect a very small area of the SNAP CCD, only 1.13×10^{-4} for a dose of 2×10^{10} protons/cm^2 assuming a threshold of 100 e^- in a ten minute exposure. Scaling this result to the dose expected in the worst case scenario, we expect a fraction 1.91×10^{-5} of the pixels to be contaminated by dark current spikes in orbit at L2. Considering the 3512×3512 layout of the SNAP CCDs, this level of contamination is equivalent to a single column defect only 235 pixels long. The SNAP observing strategy implements a dither pattern to cover gaps between detectors, equivalent to several hundred columns in width. The contribution from both column defects and hot pixels will be minor relative to the spacing between detectors, and the dither pattern will be sufficient to cover any detector area lost due to these defects.

Finally, we interpret the level of dark current following irradiation in the context of the SNAP mission. Ideally, the dominant background in SNAP observations will come from the sky itself, with the dark current generation in the CCDs playing only a minor role. Simulations predict a zodiacal background of 500 e^-/hr around 400 nm and 1300 e^-/hr at 1000 nm for the current filter design [13]. We estimate the expected level of dark current after five years by taking the constant term without annealing, and scaling the dose to the predicted levels from SPENVIS. In the worst case scenario with no anneal, the dark current of 90 e^-/hr is significantly lower than the minimum level of zodiacal. Assuming Poisson statistics, this level of dark current will only increase the RMS contribution from the background by 9% for the bluest filter. The situation only improves after an anneal, or when the nominal exposure is considered. Dark current due to radiation exposure is therefore not expected to degrade the sensitivity of SNAP observations of SNe or weak lensing shear.

VII. CONCLUSION

The behavior of thick, fully depleted, p-channel LBNL CCDs has been investigated following irradiation at the 88-inch cyclotron. We have performed extensive tests of charge transfer efficiency, generation of dark current, and hot pixels introduced from bulk damage of high energy proton exposure. A summary of the results scaled to the expected exposure at L2 can be found in Table IV.

TABLE IV

EXPECTED CCD PERFORMANCE AFTER 5 YEARS AT L2

Quantity	Pre-irrad	Worst Case Dose	Nominal Dose
Defect Pixels	< 0.001	1.9×10^{-5}	3.2×10^{-6}
Dark Current	$3-4$ e^-/hr	90 e^-/hr	15 e^-/hr
Serial CTE	0.999 999	0.999 978	0.999 996
Parallel CTE	0.999 999	0.999 991	0.999 998

The radiation studies show that the LBNL CCDs designed for use in the SNAP satellite should suffer from negligible contamination from dark current or hot pixels during the course of a five year mission. Additional effort is still required to quantify the impact of the degraded CTE performance on science observations. However, it appears that the significant improvements over n-channel CCDs currently in use in space-based observatories make these LBNL CCDs an excellent choice for use in future space-based missions like SNAP.

ACKNOWLEDGMENT

This work was sponsored by the United States Department of Energy under contract No. DE-AC02-05CH11231.

REFERENCES

[1] G. Aldering et al., "Supernova / Acceleration Probe: A Satellite Experiment to Study the Nature of the Dark Energy", astro-ph/0405232, 2004.

[2] S. E. Holland, C. J. Bebek, K. S. Dawson, J. H. Emes, M. H. Fabricius, J. A. Fairfield, D. E. Groom, A. Karcher, W. F. Kolbe, N. P. Palaio, N. A. Roe, and G. Wang, "High-voltage-compatible, fully depleted CCD development", SPIE, 6276, 10H, 2006.

[3] D. E. Groom, C. J. Bebek, M. Fabricius, A. Karcher, W. F. Kolbe, N. A. Roe, and J. Steckert, "Quantum efficiency characterization of back-illuminated CCDs Part 1: The Quantum Efficiency Machine,", SPIE, 6068, 2006.

[4] M. H. Fabricius, C. J. Bebek, D. E. Groom, A. Karcher, and N. A. Roe, "Quantum efficiency characterization of back-illuminated CCDs Part 2: Reflectivity measurements", SPIE, 6068, 2006.

[5] C. J. Bebek, D. E. Groom, S. E. Holland, A. Karchar, W. F. Kolbe, M. E. Levi, N. P. Palaio, B. T. Turko, M. C. Uslenghi, M. T. Wagner, and G. Wang, "Proton radiation damage in high-resistivity n-type silicon CCDs", SPIE 4669, 161-171, 2002.

[6] M. A. Xapsos, J. L. Barth, E. G. Stassinopoulos, E. A. Burke and G. B. Gee, "Space Environment Effects Model for Emission of Solar Protons (ESP) Cumulative and Worst Case Event Fluences", NASA/TP-1999-209763, 1999.

[7] http://www.spenvis.oma.be

[8] I. Jun, M. A. Xapsos, S. R. Messenger, E. A. Burke, R. J. Walters, G. P. Summers, and T. Jordan, "Proton nonionizing energy loss (NIEL) for device applications", NSS-IEEE, 50, 1924, 2003.

[9] C. Marshall, P .W. Marshall, A. Waczynski, E. Polidan, S. J. Johnson, and A. Campbell, "Comparisons of the proton-induced dark current and charge transfer efficiency responses of n- and p-channel CCDs", SPIE, 5499, 542, 2004.

[10] M. Bautz, G. Prigozhin, S. Kissel, B. LaMarr, C. Grant, and S. Brown, "Anomalous annealing of a high-resistivity CCD irradiated at low temperature", NSS-IEEE, 52, 519, 2005.

[11] E. J. Polidan, A. Waczynski, P. W. Marshall, S. J. Johnson, C. Marshall, R. Reed, R. A. Kimble, G. Delo, D. Schlossberg, A. M. Russell, T. Beck, Y. Wen, J. Yagelowich, R. J. Hill, and E. Wassell, "A study of hot pixel annealing in the Hubble Space Telescope Wide Field Camera 3 CCDs", SPIE, 5167, 258, 2004.

[12] M. Sirianni, M. Mutchler, M. Clampin, H. C. Ford, G. D. Illingworth, G. F. Hartig, D. van Orsow and T. Wheeler, "Performance of the Advanced Camera for Surveys CCDs after two years on orbit", SPIE, 5499, 173, 2004.

[13] T. M. Davis, B. P. Schmidt, and A. G. Kim, "Ideal Bandpasses for Type Ia Supernova Cosmology", PASP, 118, 205, 2006.